# Leptoquarks at $e\gamma$ colliders

Hélène Nadeau and David London
*Laboratoire de Physique Nucléaire, Université de Montréal, Case Postale 6128, Montréal, Québec, Canada H3C 3J7*
(Received 8 January 1993)

We consider single production of leptoquarks (LQ's) at $e\gamma$ colliders for two values of the center-of-mass energy: $\sqrt{s}=500$ GeV and 1 TeV. LQ's with masses essentially up to the kinematic limit can be seen, even for couplings as weak as $\sim(10^{-3}-10^{-2})\alpha_{\rm em}$. It is possible to detect LQ's of mass greater than $\sqrt{s}$ by looking for signals of virtual LQ production in $e\gamma\to eq\bar{q}$.

PACS number(s): 14.80.Pb, 12.10.Dm, 13.10.+q

One of the colliders planned for the coming decade is the Next Linear Collider (NLC),[1] a linear $e^+e^-$ collider with a center-of-mass energy in the range of about 500 GeV–1 TeV. This will provide a very clean environment in which to look for and study new physics not found in the standard model (SM). Some time ago it was noted [1] that these machines could be transformed into $e\gamma$ or $\gamma\gamma$ colliders of roughly the same energy and luminosity by backscattering laser light from one or both electron beams. Work has already begun which looks at the prospects for the observation of new physics in $e\gamma$ and $\gamma\gamma$ collisions.

In this paper we consider the $e\gamma$ option and investigate the possibilities for detecting leptoquarks (LQ's) at such a machine. Leptoquarks appear in a large number of extensions of the SM such as grand unified theories (GUT's), technicolor, and composite models. In general, these particles can have either spin 0 or spin 1, but here we consider only scalar (spin-0) LQ's. There are four possible leptoquark charges: $Q_{\rm em}=-\frac{1}{3}$, $-\frac{2}{3}$, $-\frac{4}{3}$, and $-\frac{5}{3}$. These correspond to the decays of the LQ into $e^-u$, $e^-\bar{d}$, $e^-d$, and $e^-\bar{u}$, respectively. For the charge $-\frac{1}{3}$ and $-\frac{2}{3}$ LQ's, there may be other decay modes, such as $\nu d$ or $\bar{\nu}d$ and $\nu\bar{u}$ or $\bar{\nu}\bar{u}$.

The leptoquarks most commonly considered in the literature are those with $Q_{\rm em}=-\frac{1}{3}$. These LQ's appear, for example, in $E_6$ superstring-inspired grand unified theories [2]. If these leptoquarks are light (i.e., observable at collider energies), then a large fraction of the parameter space of their couplings has already been ruled out [3]. Couplings of the LQ and the lepton-quark pair which are flavor violating will typically lead to low-energy flavor-changing neutral currents (FCNC's), and are hence constrained to be small. Thus, the only allowed sizable LQ couplings are those which are flavor diagonal. This implies that only leptoquarks which couple to first-generation particles can be usefully studied at an $e\gamma$ collider, since the LQ's necessarily interact with the electron in these collisions. In addition, in order to evade constraints from rare pion decays such as $\pi^+\to e^+\nu_e$, the couplings of such LQ's must be chiral. Finally, a comparison of the Fermi constants extracted from $\mu$ and $\beta$ decay (quark-lepton universality) requires that the couplings of the left-handed LQ be at most about 10% of electromagnetic strength. This is due to the fact that the LQ contribution to these processes can interfere with that of the standard model. There is an analogous constraint on the right-handed LQ coupling.

We must reiterate that the above constraints apply only to the $Q_{\rm em}=-\frac{1}{3}$ leptoquarks. They do *not* necessarily apply to LQ's of other charges. For example, many of the limits are derived using the fact that the charge $-\frac{1}{3}$ LQ couples both to $e^-u$ and $\nu_e d$. As will be seen below, the other LQ's couple either to $e^-$ and (anti)quark or $\nu_e$ and (anti)quark, but not both. Thus there is no constraint from $\pi^+\to e^+\nu_e$, for example. Nevertheless, in this paper we will follow the conventions used in the literature—we will assume that the couplings of all leptoquarks are flavor diagonal, and we will present our results in terms of the chiral couplings of all LQ's. However, the reader should be aware that the couplings of LQ's with $Q_{\rm em}\neq-\frac{1}{3}$ are not necessarily required phenomenologically to follow these patterns [4].

It might be argued that, in any event, the leptoquarks most likely to exist are those with charge $-\frac{1}{3}$ since they are the best motivated theoretically. We do not subscribe to this. In general, the $E_6$ models which predict the existence of such LQ's also predict that these particles acquire a mass of the order of the scale at which $E_6$ is broken, i.e., the GUT scale, so that there are no light LQ's. It may be possible to concoct variants in which additional *ad hoc* discrete symmetries are introduced which keep the LQ's light, but these are not particularly well motivated. Instead, we take, and we encourage the experimentalists to take, a more model-independent point of view, and consider the production of leptoquarks of all charges, both real and virtual, at an $e\gamma$ collider.

Leptoquark production at $e^+e^-$, $p\bar{p}$, and $ep$ colliders has also been discussed in the literature. Results from the CERN $e^+e^-$ collider LEP imply that the LQ mass is greater than $M_Z/2$ [5]. This could be extended to $\sim 80$

[1]By NLC, we mean any of the linear colliders which are now being discussed [KEK Japan Linear Collider (JLC), Serpukhov VLEPP, NLC and/or TeV Linear Collider (TLC), CERN Linear Collider (CLIC), Cornell TeV Energy Superconducting Linear Accelerator (TESLA), . . .].

 

GeV by looking for single leptoquarks [6]. The limits from UA2 depend somewhat on the coupling strength, but give a lower bound on LQ masses of about 70 GeV [7]. The DESY $ep$ collider HERA is ideally suited to the search for leptoquarks, and it is expected that, for a large range of couplings, LQ's with masses up to the kinematic limit can be seen [8,9,10]. As we will show, $e\gamma$ colliders are also very useful tools in searching for light leptoquarks, since these can be produced singly in such experiments. Single leptoquark production in $e\gamma$ collisions has been considered by Hewett and Pakvasa [11] in the context of $e^+e^-$ colliders. We will apply their results specifically to $e\gamma$ colliders and extend them to include the possibility of single virtual leptoquark production.

Buchmüller *et al.* [8] have written down the most general SU(3)×SU(2)×U(1) invariant scalar leptoquark couplings which satisfy baryon and lepton number conservation. Defining the fermion number $F=3B+L$, where $B$ is baryon number and $L$ is lepton number, it is possible to have leptoquarks whose couplings obey $|\Delta F|=0$ or 2 (we follow the notation of Ref. [6]):

$$\begin{aligned}\mathcal{L}_{|\Delta F|=2}&=g_{1L}\overline{q_L^c}\,i\tau_2 l_L S_1+g_{1R}\overline{u_R^c}\,e_R S_1'\\&\quad+\tilde{g}_{1R}\overline{d_R^c}\,e_R\tilde{S}_1+g_{3L}\overline{q_L^c}\,i\tau_2\tau^i l_L S_3^i\ ,\\\mathcal{L}_{|\Delta F|=0}&=h_{2L}\bar{u}_R l_L R_2+h_{2R}\bar{q}_L i\tau_2 e_R R_2'\\&\quad+\tilde{h}_{2L}\bar{d}_R l_L\tilde{R}_2\ ,\end{aligned}\tag{1}$$

where $q_L$ and $l_L$ are the standard left-handed $SU(2)_L$ doublets of quarks and leptons, respectively, and $\psi^c=C\bar{\psi}^T$ is a charge-conjugated fermion field. The leptoquarks $S_1$, $S_1'$, and $\tilde{S}_1$ are $SU(2)_L$ singlets, $R_2$, $R_2'$, and $\tilde{R}_2$ are $SU(2)_L$ doublets, and $S_3$ is an $SU(2)_L$ triplet.

Only those LQ's which couple to electrons can be produced, either as real or virtual particles, in $e\gamma$ collisions. There are eight such types, distinguished by the (anti)quark which is produced along with the (real or virtual) leptoquark in the final state, as well as the chirality of the LQ coupling (chirality here is defined as the helicity of the electron). These are listed in Table I.

TABLE I: The eight types of leptoquark ($S$) which can be produced in $e\gamma$ collisions. The $S$ can be real or virtual. The "chirality" refers to the helicity of the $e^-$—either left handed (LH) or right handed (RH).

| Process | $Q_S$ | Chirality | Origin |
|---|---|---|---|
| $e^-\gamma\to S\bar{u}$ | $-\frac{1}{3}$ | LH | $S_1,S_3$ |
| $e^-\gamma\to S\bar{u}$ | $-\frac{1}{3}$ | RH | $S_1'$ |
| $e^-\gamma\to S\bar{d}$ | $-\frac{4}{3}$ | LH | $S_3$ |
| $e^-\gamma\to S\bar{d}$ | $-\frac{4}{3}$ | RH | $\tilde{S}_1$ |
| $e^-\gamma\to Su$ | $-\frac{5}{3}$ | LH | $R_2$ |
| $e^-\gamma\to Su$ | $-\frac{5}{3}$ | RH | $R_2'$ |
| $e^-\gamma\to Sd$ | $-\frac{2}{3}$ | LH | $\tilde{R}_2$ |
| $e^-\gamma\to Sd$ | $-\frac{2}{3}$ | RH | $R_2'$ |

Let us first turn to real leptoquark production. The diagrams which are responsible for single LQ production in $e\gamma$ collisions are shown in Fig. 1. For the production of real leptoquarks, the chirality of the coupling is irrelevant. The cross sections which we will calculate are equal for left-handed and right-handed leptoquarks. (Of course, if a leptoquark were detected, electron polarization could be used to ascertain its origin.) In this case, there are essentially four types of LQ, distinguished by their electromagnetic charge. These four types of LQ can be compared by simply keeping the charge of the leptoquark, $Q_S$, as a parameter in the calculations of the diagrams of Fig. 1.

Replacing the couplings $g_{1L},\ldots,\tilde{h}_{2L}$ of Eq. (1) by a generic leptoquark Yukawa coupling $g$, we conventionally parametrize $g$ by scaling it to electromagnetic strength, $g^2/4\pi=k\alpha_{\rm em}$, and allow $k$ to vary. With this notation, the differential cross section for the diagrams of Fig. 1 is then found to be

$$\begin{aligned}\frac{d\sigma}{du}=-\frac{\pi k\alpha_{\rm em}^2}{2s^2}\Bigg\{&-\frac{u}{s}-2Q_S^2\frac{u(u+s-M_S^2)^2}{s(u+s)^2}-2Q_S\frac{u(u+s-M_S^2)}{s(u+s)}-(1+Q_S)^2\left[\frac{s}{u}+2\frac{(u-M_S^2)(u+s-M_S^2)}{su}\right]\\&+2(1+Q_S)\frac{u-M_S^2}{s}+4Q_S(1+Q_S)\frac{(u+s-M_S^2)(s/2+u-M_S^2)}{s(u+s)}\Bigg\},\end{aligned}\tag{2}$$

in which $u=-s\beta\frac{1}{2}(1+\cos\theta)$, with $\beta=1-M_S^2/s$. (We note that this expression agrees with that of Ref. [11] for $Q_S=-\frac{1}{3}$, with the replacement $k\to 2k$. This change in $k$ is due to a difference of $\sqrt{2}$ between us and the authors of Ref. [11] in the definition of the LQ coupling of Eq. (1).)

In fact, Eq. (2) can be integrated analytically. Including a $p_T$ cut on the associated jet of $p_{T_{\rm jet}}>10$ GeV, we present the results in Fig. 2, for two values of $\sqrt{s}$, 500 GeV and 1 TeV, for each of the four LQ charges, with $k=1$. The LQ's with charge $-\frac{5}{3}$ and $-\frac{1}{3}$, which couple the electron to $\bar{u}$ or $u$ quarks, have larger cross sections than the charge $-\frac{4}{3}$ and $-\frac{2}{3}$ LQ's, which couple to $\bar{d}$ or $d$ quarks. This is due to the difference of the quark charges, which is important in Fig. 1(c). The charge of the LQ's themselves play a role [see Fig. 1(b)], as can be seen by the fact that the charge $-\frac{5}{3}$ LQ has a larger cross section than the charge $-\frac{1}{3}$ LQ, and similarly for the other two charges. This effect is of course largest for light leptoquarks, where the diagrams in Fig. 1(b) is particularly important. The expected luminosity at the NLC is 10 fb$^{-1}$ at 500 GeV, and 60 fb$^{-1}$ at 1 TeV. Thus, depending on the charge of the leptoquark, one expects somewhere between ~200 and ~6000 events for $k=1$, for the LQ mass up to essentially the kinematic limit.

Except for the left-handed charge $-\frac{1}{3}$ LQ's $S_1$ and $S_3$, all the leptoquarks in Table I decay exclusively to $eq$ or

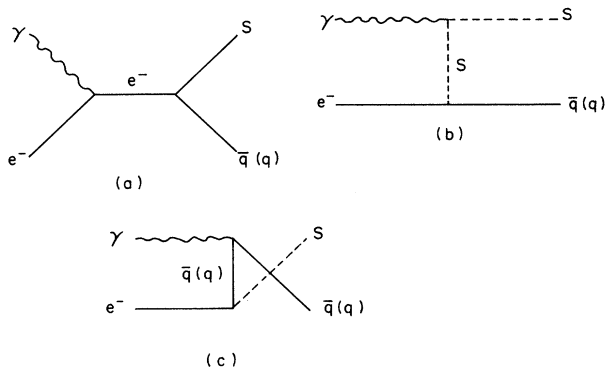


FIG. 1. Diagrams contributing to single leptoquark ($S$) production in $e\gamma$ collisions. The final state contains a $q$ if the LQ has fermion number $F=0$ and a $\bar{q}$ if $F=2$.

$e\bar{q}$, so the final state will be an electron and 2 jets. $S_1$ and $S_3$ can also decay to $\nu d$, which gives a final state of 2 jets and missing energy. Both of these final states, $ejj$ and $\not{p}_T jj$, can be produced via standard model processes, namely, $e\gamma \to eZ \to ejj$ and $e\gamma \to \nu W \to \not{p}_T jj$. However, these will cause no problems. First of all, the leptoquark signal includes a sharp invariant mass peak in $M_{ej}$ or $M_{\not{p}_T j}$ at $M_S$, which is not present in the SM decays. Rather, the SM processes will produce mass peaks in $M_{jj}$ at $M_Z$ or $M_W$ (which are absent in the case of leptoquark production). Also, in $W$ or $Z$ decay, the jets will tend to be collinear, while the jets in leptoquark decay will be widely separated. Thus, a simple cut on the angle between the jets should eliminate essentially all the background, and so the discovery limit is simply set by the signal rate. This means that LQ's whose coupling strength is considerably weaker than electromagnetic can be detected. This is made more quantitative in Fig. 3,

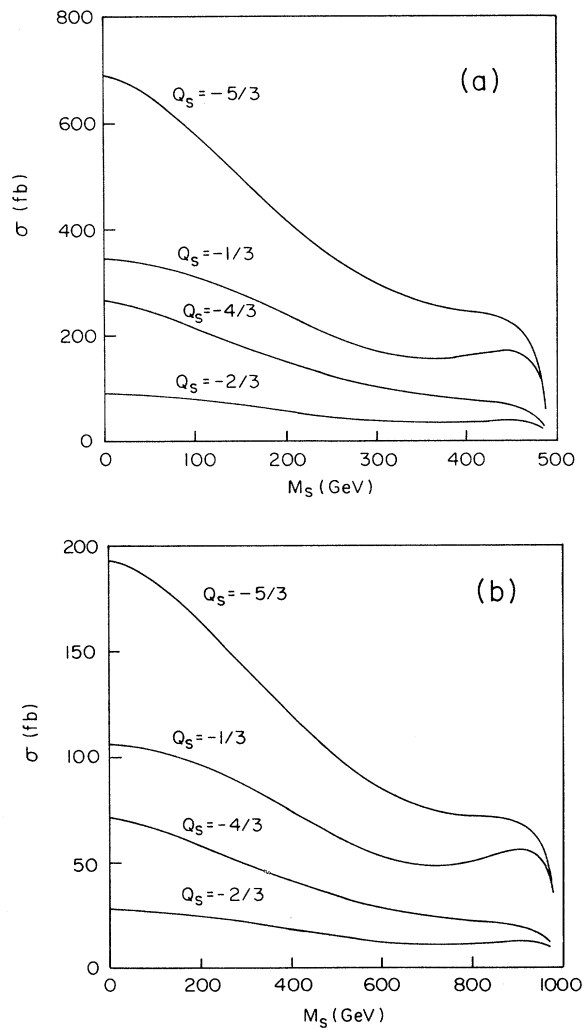


FIG. 2. Cross section for single leptoquark production in $e\gamma$ collisions at (a) $\sqrt{s}=500$ GeV, (b) $\sqrt{s}=1$ TeV, for the four possible LQ charges, $Q_S=-\frac{1}{3}, -\frac{2}{3}, -\frac{4}{3}, -\frac{5}{3}$. The results are given for $k=1$.

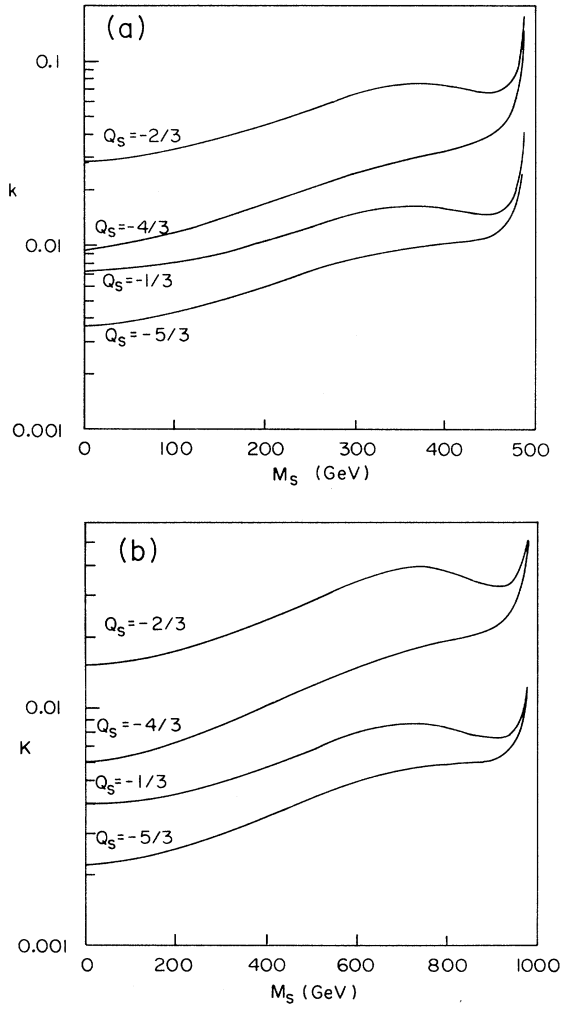


FIG. 3. Discovery region (25 events) for leptoquarks as a function of their mass ($M_S$) and coupling strength ($k$), in $e\gamma$ collisions at (a) $\sqrt{s}=500$ GeV, (b) $\sqrt{s}=1$ TeV, for the four possible LQ charges, $Q_S=-\frac{1}{3}, -\frac{2}{3}, -\frac{4}{3}, -\frac{5}{3}$. For a given curve, the parameter space above the curve is observable.

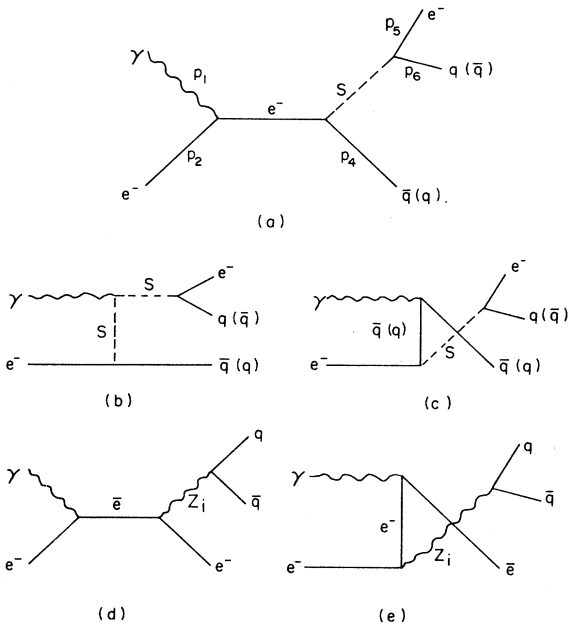


FIG. 4. Diagrams for the process $e\gamma \to eq\bar{q}$. The LQ diagrams are (a),(b),(c); the SM diagrams are (d),(e). If the virtual LQ has fermion number $F=0$, then the $q/\bar{q}$ assignments are those given in parentheses; if $F=2$, they are not in parentheses. The momentum assignments for all five diagrams are given in (a). Note that, regardless of $F$, $p_4$ is assigned to the line which is connected to the initial $e$.

where we plot the discovery limits (defined as 25 events) as a function of $M_S$ and $k$ for each of the 4 charges of leptoquark. From this figure it is seen that leptoquarks with $k$ as small as $\sim 10^{-3}$–$10^{-2}$ can be detected for most of the kinematically allowed mass range.

One can try to go beyond the kinematic limit by considering virtual single leptoquark production, as shown in Figs. 4(a)–4(c). The problem here is that the process of interest is $e\gamma \to eq\bar{q}$, which has an enormous standard model background [Figs. 4(d) and 4(e)]. It is therefore necessary to calculate the cross section for this process including all the diagrams of Fig. 4, and to look for a set of cuts which reduces the SM contribution to a level where the presence of leptoquarks is observable. This is what we have done. We will see that it is possible to detect LQ's whose mass is greater than the kinematic limit, but to go well beyond this limit requires that $k > 1$, i.e., that the coupling be stronger than that of the electromagnetic interaction.

The cross section is calculated for all eight types of LQ shown in Table I. We will keep track of the charge of the leptoquark as in the previous calculation of real leptoquark production. As to the LQ chirality, it is important only in the interference of the leptoquark and SM diagrams—it indicates which of the left- and right-handed couplings of the photon/$Z$ is selected in these terms. For example, the right-handed charge $-\frac{1}{3}$ LQ couples to right-handed electrons and right-handed $u$ quarks, thus, only the SM diagrams with right-handed couplings will interfere with the LQ diagrams.

There is one technical point regarding the calculation. The momentum assignments of the initial and final-state particles are shown in Fig. 4(a). As is evident from this figure, the momenta of the final quark and antiquark depend on whether the leptoquark has fermion number $F=0$ or 2. The LQ's of charge $-\frac{2}{3}$ and $-\frac{5}{3}$ have fermion number 0, while those with $Q_{\rm em}=-\frac{1}{3}$ and $-\frac{4}{3}$ have $F=2$. If $F=0$, the quark has momentum $p_4$ and the antiquark $p_6$, while for $F=2$, these are switched. As far as the leptoquark diagrams are concerned, this is irrelevant, but it is important for the SM contribution. We take this point into account in the expressions below.

The contribution to the total cross section for $e\gamma \to eq\bar{q}$ which is due solely to leptoquarks [Figs. 4(a)–4(c)] is calculated to be

$$\frac{1}{4}\sum_{\rm spins}|\mathcal{M}_{\rm LQ}|^2$$

$$=128\pi^3 k^2\alpha_{\rm em}^3\frac{p_5\cdot p_6}{[2p_5\cdot p_6-M_S^2]^2}\left\{\frac{p_1\cdot p_4}{s}+8Q_S^2\frac{p_1\cdot p_4(p_2\cdot p_4)^2}{s[2p_2\cdot p_4+M_S^2]^2}+\frac{1}{4}(1+Q_S)^2\frac{s}{p_1\cdot p_4}\left[1+8\left[p_2\cdot p_4-\frac{s}{2}\right]\frac{p_2\cdot p_4}{s^2}\right]\right.$$
$$+4Q_S\frac{p_1\cdot p_4 p_2\cdot p_4}{s[2p_2\cdot p_4+M_S^2]}-(1+Q_S)\left[1-2\frac{p_2\cdot p_4}{s}\right]$$
$$\left.-2Q_S(1+Q_S)\frac{p_2\cdot p_4}{2p_2\cdot p_4+M_S^2}\left[1-4\frac{p_2\cdot p_4}{s}\right]\right\}, \tag{3}$$

where $M_S$ is the mass of the leptoquark, $Q_S$ is its charge, and the momenta $p_1$–$p_6$ are defined in Fig. 4(a).

The SM diagrams [Figs. 4(d) and 4(e)] include the contributions of both the photon and the $Z$, which we will denote $Z_0$ and $Z_1$, respectively. Writing the $Z_i f\bar{f}$ couplings as

$$-ie(v_i^f\gamma^\mu-a_i^f\gamma^\mu\gamma_5)\,, \tag{4}$$

it is useful to define

$$B_{ij}\equiv(v_i^q v_j^q+a_i^q a_j^q)(v_i^e v_j^e+a_i^e a_j^e)\ ,\quad E_{ij}\equiv(v_i^q a_j^q+a_i^q v_j^q)(v_i^e a_j^e+a_i^e v_j^e)\ , \tag{5}$$

where $q=d,u$ and $i,j=0,1$. We also define

$$A_{ij}\equiv\frac{(p_3^2-M_i^2)(p_3^2-M_j^2)+(\Gamma_i M_i)(\Gamma_j M_j)}{[(p_3^2-M_i^2)^2+(\Gamma_i M_i)^2][(p_3^2-M_j^2)^2+(\Gamma_j M_j)^2]}\ , \tag{6}$$

where $i,j=0,1$ and $p_3^2=(p_4+p_6)^2$. The SM contribution to the cross section $e\gamma\to eq\bar{q}$ is then

$$\begin{aligned}\frac{1}{4}\sum_{\text{spins}}|\mathcal{M}_{\text{SM}}|^2 &= \frac{1024\pi^3\alpha_{\text{em}}^3}{s}\sum_{ij}A_{ij}\left[B_{ij}\frac{1}{p_1\cdot p_5}(s\epsilon_k\cdot p_4\epsilon_k\cdot p_6 p_1\cdot p_5+sp_1\cdot p_5 p_4\cdot p_6+2p_1\cdot p_4 p_1\cdot p_6 p_2\cdot p_5)\right.\\ &\quad+[B_{ij}-(-1)^{(F/2)}E_{ij}]\left\{p_1\cdot p_4 p_5\cdot p_6+\frac{1}{2(p_1\cdot p_5)}[s\epsilon_k\cdot p_4\epsilon_k\cdot p_5 p_6\cdot(p_5-p_1)-sp_1\cdot p_6 p_4\cdot p_5\right.\\ &\quad-2p_1\cdot p_4 p_1\cdot p_5 p_2\cdot p_6]\\ &\quad+\frac{s}{2(p_1\cdot p_5)^2}[(\epsilon_k\cdot p_5)^2 p_2\cdot p_4 p_6\cdot(p_5-p_1)+\epsilon_k\cdot p_5\epsilon_k\cdot p_6 p_1\cdot p_5 p_2\cdot p_4\\ &\quad\left.+p_1\cdot p_5 p_1\cdot p_6 p_2\cdot p_4]\right\}+[B_{ij}+(-1)^{(F/2)}E_{ij}]\\ &\quad\times\left\{p_1\cdot p_6 p_4\cdot p_5+\frac{1}{2(p_1\cdot p_5)}[s\epsilon_k\cdot p_5\epsilon_k\cdot p_6 p_4\cdot(p_5-p_1)-sp_1\cdot p_4 p_5\cdot p_6-2p_1\cdot p_6 p_1\cdot p_5 p_2\cdot p_4]\right.\\ &\quad\left.\left.+\frac{s}{2(p_1\cdot p_5)^2}[(\epsilon_k\cdot p_5)^2 p_2\cdot p_6 p_4\cdot(p_5-p_1)+\epsilon_k\cdot p_4\epsilon_k\cdot p_5 p_1\cdot p_5 p_2\cdot p_6+p_1\cdot p_4 p_1\cdot p_5 p_2\cdot p_6]\right\}\right]\ ,\end{aligned} \tag{7}$$

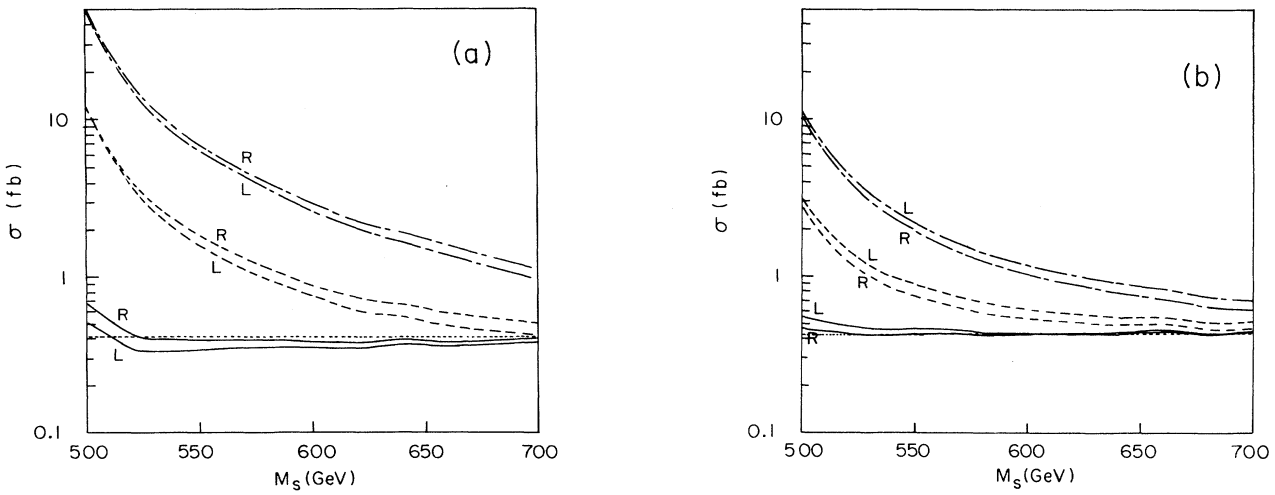


FIG. 5. Total cross section for $e\gamma\to eq\bar{q}$ at $\sqrt{s}=500$ GeV, including both LQ and SM contributions, for (a) $Q_S=-\frac{1}{3}$, (b) $Q_S=-\frac{2}{3}$, (c) $Q_S=-\frac{4}{3}$, and (d) $Q_S=-\frac{5}{3}$, for both left-handed ($L$) and right-handed ($R$) leptoquarks. The solid line has $k=1$, the dashed line has $k=5$, and the dash-dot line has $k=10$. The SM prediction is the dotted line, and is 0.42 fb in (a),(d) and 0.43 fb in (b),(c).

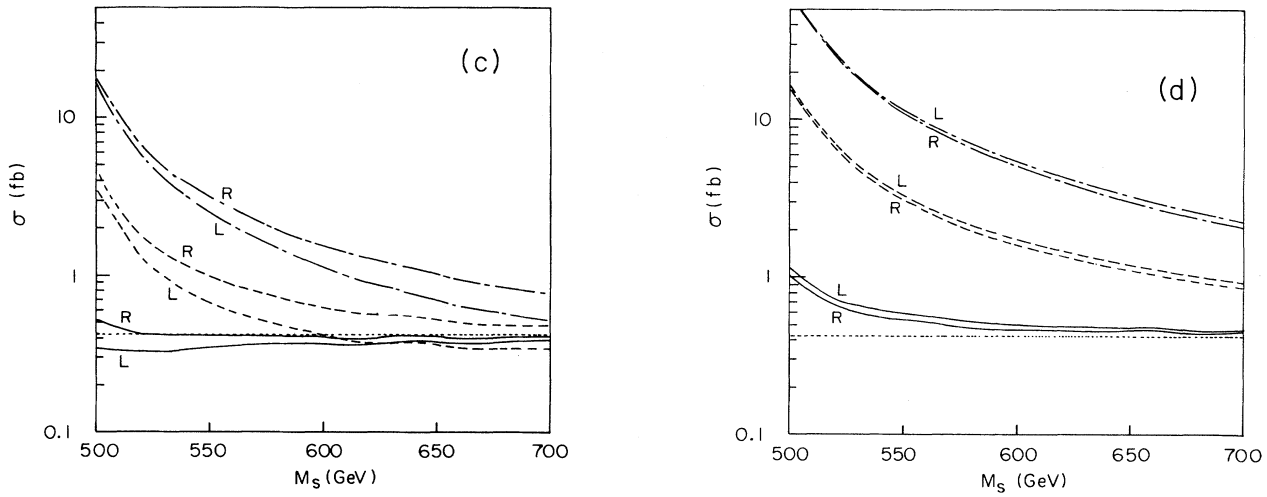


FIG. 5. (*Continued*).

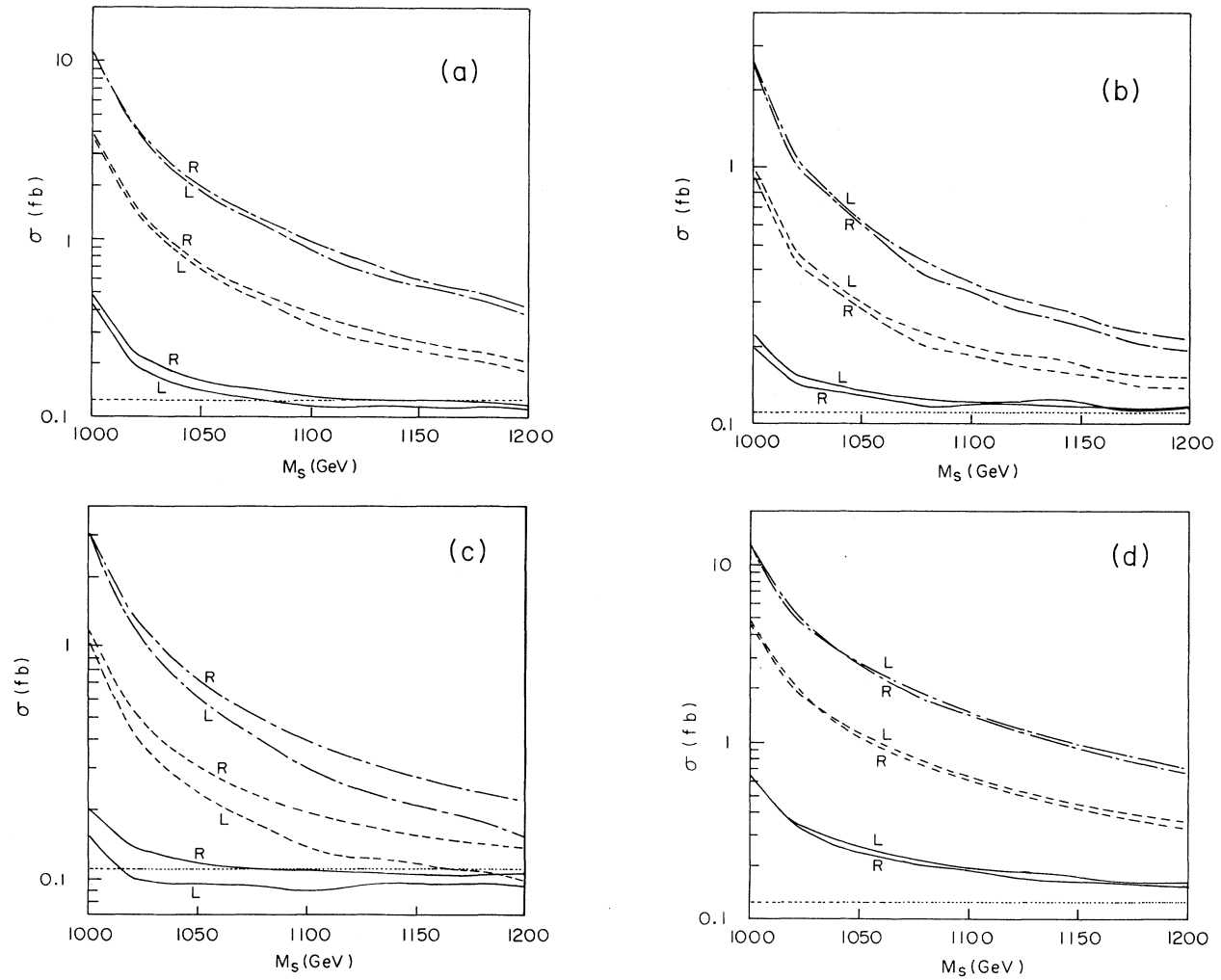


FIG. 6. Total cross section for $e\gamma \to eq\bar{q}$ at $\sqrt{s} = 1$ TeV, including both LQ and SM contributions, for (a) $Q_S = -\frac{1}{3}$, (b) $Q_S = -\frac{2}{3}$, (c) $Q_S = -\frac{4}{3}$, and (d) $Q_S = -\frac{5}{3}$, for both left-handed ($L$) and right-handed ($R$) leptoquarks. The solid line has $k = 1$, the dashed line has $k = 3$, and the dash-dot line has $k = 5$. The SM prediction is the dotted line, and is 0.13 fb in (a),(d) and 0.11 fb in (b),(c).

where $F$ is the fermion number of the leptoquark (as discussed above, the fermion number of the leptoquark defines the momenta of the quark and antiquark). The $\epsilon_k$ are the two polarizations of the initial photon. In the above expression, wherever two $\epsilon_k$'s appear, a sum over $k=1,2$ is implicit.

Finally, the interference terms between the LQ and SM diagrams remain to be calculated. As noted earlier, either the left- or right-handed SM couplings to the electron and quark contribute in this interference, but not both. It is the leptoquark chirality which dictates which SM couplings are selected. Denoting by $h_e$ ($h_q$) the helicity of the electron (quark) to which the LQ couples [i.e., $h_e(h_q)=L$ or $R$, depending on the leptoquark], the contribution to the cross section due to the interference terms is found to be

$$\begin{aligned}
&\frac{1}{4}\sum_{\text{spins}}|\mathcal{M}_{\text{int}}|^2 \\
&\quad=\frac{2048\pi^3 k\alpha_{\text{em}}^3}{2p_5\cdot p_6-M_S^2}\sum_i c_{ih_e}^e c_{ih_q}^q \frac{(2p_4\cdot p_6-M_i^2)}{(2p_4\cdot p_6-M_i^2)^2+M_i^2\Gamma_i^2} \\
&\qquad\times\left[\frac{p_1\cdot p_4 p_5\cdot p_6}{s}-\frac{1}{4p_1\cdot p_5}\frac{1}{s}(s\epsilon_k\cdot p_4\epsilon_k\cdot p_5(p_1-p_5)\cdot p_6+s[p_1\cdot p_6 p_4\cdot p_5-p_1\cdot p_5 p_4\cdot p_6]\right. \\
&\qquad\qquad -s\epsilon_k\cdot p_4\epsilon_k\cdot p_6 p_1\cdot p_5+2p_1\cdot p_4[p_1\cdot p_5 p_2\cdot p_6-p_1\cdot p_6 p_2\cdot p_5]) \\
&\qquad+\frac{1}{2}Q_s\frac{1}{2p_2\cdot p_4+M_S^2}\left[(\epsilon_k\cdot p_4)^2 p_5\cdot p_6+\frac{p_2\cdot p_4}{p_1\cdot p_5}\epsilon_k\cdot p_4[\epsilon_k\cdot p_6 p_1\cdot p_5+\epsilon_k\cdot p_5(2p_5-p_1)\cdot p_6]\right] \\
&\qquad-\frac{1}{4}(Q_S+1)\frac{p_5\cdot p_6}{p_1\cdot p_4}[2p_1\cdot p_4-(\epsilon_k\cdot p_4)^2]+\frac{1}{4}(Q_S+1)\frac{1}{p_1\cdot p_4 p_1\cdot p_5}[\epsilon_k\cdot p_4\cdot\epsilon_k\cdot p_6 p_1\cdot p_5(p_4-p_1)\cdot p_2 \\
&\qquad+\epsilon_k\cdot p_4\cdot\epsilon_k\cdot p_5(p_2\cdot p_4 p_5\cdot p_6+p_2\cdot(p_1-p_4)p_6\cdot(p_1-p_5)) \\
&\qquad\left.+p_1\cdot p_4(p_1\cdot p_5 p_2\cdot p_6-p_1\cdot p_6 p_2\cdot p_5)+s(p_1\cdot p_6 p_4\cdot p_5-p_1\cdot p_5 p_4\cdot p_6)/2]\right], \qquad (8)
\end{aligned}$$

where we have neglected the width $\Gamma_i$ in the numerator. In the above equation, the standard model couplings to the electron and quark are given by $c_{ih_e}^e$ and $c_{ih_q}^q$, respectively, in which $c_{iL}^f=(v_i^f+a_i^f)/2$ and $c_{iR}^f=(v_i^f-a_i^f)/2$. As in Eq. (7), for those terms in which two $\epsilon_k$'s appear, a sum is implicit over the two photon polarizations.

The total cross section for $e\gamma\to eq\bar{q}$ is given by integrating the sum of the three expressions in Eqs. (3), (7), and (8) over the allowed phase space. This must be done by Monte Carlo calculations. It is clear that if no cuts are applied, the standard model contribution dominates by many orders of magnitude due to the fact that the gauge bosons can be on shell. We have therefore applied stringent cuts in the integration in order to considerably reduce the SM background. We have again considered two collider energies: $\sqrt{s}=500$ GeV and 1 TeV. For the 500-GeV machine we required that the $p_T$ of the electron be greater than 100 GeV, that the invariant mass of the $q\bar{q}$ be greater than 100 GeV, and that the angle between the two jets satisfy $\cos\theta_{q\bar{q}}<-0.4$. For the 1-TeV machine we used $p_T(e^-)>200$ GeV, $m_{q\bar{q}}>100$ GeV, and $\cos\theta_{q\bar{q}}<-0.2$. We also considered three different values of $k$, the LQ coupling strength, at both values of $\sqrt{s}$.

Our results, for all LQ charges and chiralities, are shown in Figs. 5 and 6. Figures 5(a)–5(d) show the cross section at $\sqrt{s}=500$ GeV, for the 4 leptoquark charges, for $k=1,5,10$. For $k=1$, the cross section with both LQ and SM contributions is essentially indistinguishable from that in which only the SM is present. However, for the larger values of $k$, it is possible to see significant deviations from the SM predictions (recall that the expected integrated luminosity is 10 fb$^{-1}$). Depending on the value of $k$, a leptoquark with a mass of 700 GeV or even greater may be observed. Note also that the left- and right-handed LQ's tend to give very similar cross sections.

The cross sections at $\sqrt{s}=1$ TeV are shown in Figs. 6(a)–6(d). Here we have taken $k=1,3,5$. Again, the curves with $k=1$ are fairly similar to the SM prediction, but this time it may be possible to see a leptoquark with a mass somewhat greater than the machine energy for some of the charges (especially $Q_{\text{em}}=-\frac{5}{3}$), given that the expected integrated luminosity is 60 fb$^{-1}$. For $k=3$ or 5, on the other hand, leptoquarks with a mass considerably larger than the kinematic limit are observable. As at $\sqrt{s}=500$ GeV, the cross sections with left- and right-handed LQ's are not very different from one another.

We remind the reader that a light ($M_S\lesssim 1$ TeV) charge $-\frac{1}{3}$ left-handed LQ must have $k<0.1$ due to low-energy phenomenological considerations. However, from Figs. 5 and 6, we see that, for both $\sqrt{s}=500$ GeV and 1 TeV, it is necessary that $k\gtrsim 1$ in order that the signal for a LQ with a mass larger than $\sqrt{s}$ be observable. Therefore the signal for this particular leptoquark is already excluded.

For this reason we have not considered the additional process $e\gamma \to \nu_e d\bar{u}$, which is possible with a virtual charge $-\frac{1}{3}$ left-handed LQ, and which also has a SM background. For $k \simeq 0.1$, the LQ contribution to this process would be much smaller than that of the SM.

From Figs. 5 and 6 it is clear that a larger energy machine is preferable if one wishes to observe signals of virtual leptoquarks. Not only can one simply probe larger masses, but smaller values of $k$ are allowed. The point is that the largest contribution to the SM background comes from that region of phase space which is nearest to the point where the gauge bosons are produced on shell. As the energy of the machine increases, harder cuts can be imposed, thereby further reducing the SM background. This is the reason that the signals for LQ's with $k > 1$ are more striking at $\sqrt{s} = 1$ TeV (Fig. 6) than at 500 GeV (Fig. 5).

To conclude, we have considered the possibility for the detection of leptoquarks at $e\gamma$ colliders with $\sqrt{s} = 500$ GeV and 1 TeV. It turns out that $e\gamma$ colliders are excellent hunting grounds for LQ's since these particles can be produced singly at such machines. Real leptoquarks can be observed with masses essentially up to the center-of-mass energy even for couplings as small as $\sim 10^{-3}$–$10^{-2}\alpha_{\rm em}$. It is possible to find evidence for the existence of LQ's with masses greater than the kinematic limit by looking for signals of virtual leptoquark production in the process $e\gamma \to eq\bar{q}$, for that region of parameter space in which the LQ coupling is stronger than $\alpha_{\rm em}$.

We would like to thank G. Bélanger, A. Djouadi, J. Hewett, and P. Langacker for helpful discussions. This work was supported in part by the Natural Sciences and Engineering Research Council of Canada, and by FCAR, Québec.

[1] I. F. Ginzburg, G. L. Kotkin, V. G. Serbo, and V. I. Telnov, Pis'ma Zh. Eksp. Teor. Fiz. **34**, 514 (1981) [JETP Lett. **34**, 491 (1981)]; Yad. Fiz. **38**, 372 (1983) [Sov. J. Nucl. Phys. **38**, 222 (1983)]; Nucl. Instrum. Methods **205**, 47 (1983); I. F. Ginzburg, G. L. Kotkin, S. L. Panfil, V. G. Serbo, and V. I. Telnov, Yad. Fiz. **38**, 1021 (1983) [Sov. J. Nucl. Phys. **38**, 614 (1983)]; Nucl. Instrum. Methods **219**, 5 (1984).

[2] J. L. Hewett and T. G. Rizzo, Phys. Rep. **183**, 193 (1989).

[3] W. Buchmüller and D. Wyler, Phys. Lett. B **177**, 377 (1986).

[4] Constraints on the parameter space of the LQ's with $Q_{\rm em} \neq -\frac{1}{3}$ are presently being studied: G. Bélanger (private communication).

[5] ALEPH Collaboration, D. Decamp *et al.*, CERN Report No. CERN-PPE/91-149, 1991 (unpublished); DELPHI Collaboration, P. Abreu *et al.*, CERN Report No. CERN-PPE/91-138, 1991 (unpublished); L3 Collaboration, B. Adeva *et al.*, Phys. Lett. B **261**, 169 (1991); OPAL Collaboration, G. Alexander *et al.*, *ibid.* **263**, 123 (1991).

[6] T. G. Rizzo, Phys. Rev. D **44**, 186 (1991).

[7] UA2 Collaboration, J. Alitti *et al.*, CERN Report No. CERN-PPE/91-158 (unpublished).

[8] W. Buchmüller, R. Rückl, and D. Wyler, Phys. Lett. B **191**, 442 (1987).

[9] V. Angelopoulos *et al.*, Nucl. Phys. **B292**, 59 (1987); J. F. Gunion and E. Ma, Phys. Lett. B **195**, 257 (1987).

[10] N. Harnew, in *Proceedings of the DESY Workshop 1987: Physics at HERA*, Hamburg, Germany, 1987, edited by R. Peccei (DESY, Hamburg, 1987).

[11] J. L. Hewett and S. Pakvasa, Phys. Lett. B **227**, 178 (1989).